

# Inundation Discriminated Using Sun Glint

Vern C. Vanderbilt, *Member, IEEE*, Guillaume L. Perry, Gerald P. Livingston, Susan L. Ustin, *Member, IEEE*, Martha C. Diaz Barrios, François-Marie Bréon, Marc M. Leroy, Jean-Yves Balois, Leslie A. Morrissey, Stanley R. Shewchuk, Joel A. Stearn, Sarah E. Zedler, Jonathan L. Syder, Sophie Bouffies-Cloche, and Maurice Herman

**Abstract**—Inundation is linked to water, carbon, and energy budgets at landscape to global scales. We describe a new remote-sensing technique for identifying inundated areas based on the properties of the glitter—the strong, angular signature reflection that is characteristic of surface water and uncharacteristic of other cover types. We discriminated three cover types—vegetation emergent above inundated soils, open water, and noninundated cover types—from analysis of directional data collected in the red spectral band by the airborne POLDER (polarization and directionality of earth's reflectance) sensor. We found that values of the normalized difference vegetation index (NDVI) decreased dramatically in the glitter direction, providing an indication of surface water. Application of our new technique holds promise for mapping the seasonal and interannual extent of inundation, a key descriptor of wetlands hydrology.

**Index Terms**—Bidirectional reflectance, bidirectional reflectance distribution function (BRDF), inundation, methane, specular reflection of sunlight, wetlands.

## I. INTRODUCTION

### A. Remote Sensing of Inundation

GLOBAL mapping of areas inundated by water remains an important and unachieved goal of remote-sensing research tied to climate change and terrestrial biospheric function [1]–[3]. An accurate, satellite-based approach capable of monitoring the extent of inundated areas is needed to improve understanding of seasonal and interannual wetlands hydrology [4].

Inundation is a key hydrologic variable in budgets for water and carbon [4]–[6]. Estimates of both inundated and

noninundated land areas provide information to carbon budgets representing the exchange of the two trace gases, carbon dioxide and methane, between the soil and the atmosphere at local to global scales [4]. Inundated anaerobic soil is a potential source of methane, while noninundated aerobic soil is a potential source of carbon dioxide and a sink for methane [7], [8]. The increases in the concentrations of these gases in the atmosphere have been linked to potential changes in earth's climate. Inundation is an important factor in energy budgets, modifying rates of water evaporation and transpiration and the thermal conductivity and thermal insulating properties of the inundated area [9]–[13].

Despite its importance to the functioning of earth's terrestrial biosphere, globally consistent estimates of the areal extent of inundation are nonexistent. Estimates have been derived from a variety of sources with various spatial and temporal scales and usually have been limited to specific regions [14]–[16]. The potential of spaceborne microwave instruments to map inundated areas has been identified but remains to be realized at the global scale [17], [18]. Similarly, application of optical remote-sensing methods has met with mixed success [4], [16], [19], [20].

### B. Hypotheses Tested

We present results of a proof-of-concept study to estimate the extent of inundation from analysis of airborne POLDER (polarization and directionality of earth's reflectance) [21] data collected in support of the BOREAS Experiment [22], [23] in central Saskatchewan, Canada. We believe this is the first study to take advantage of the specular reflecting properties of surface waters [24]–[26] to discriminate inundated areas (with emergent vegetation), open water (without emergent vegetation), and noninundated cover types.

We tested three hypotheses. First, the glitter of sunlight off water surfaces provides a strong, angular signature reflection characteristic of inundated areas and uncharacteristic of noninundated cover types. Second, open water areas and inundated areas display different, wind-dependent glitter signatures as a function of view angle. Third, analysis of remotely sensed data, collected in and near the specular direction, allows accurate discrimination of inundated areas, open water, and noninundated cover types.

## II. METHODS

### A. Data Collection

Radiance images were collected above the BOREAS Southern Study Area (SSA), in central Canada (54°N, 105°W) near Prince Albert, Saskatchewan, using POLDER, a large

Manuscript received December 18, 2000; revised February 14, 2002.

V. C. Vanderbilt is with the Ames Research Center, Moffett Field, CA 94035 USA.

G. L. Perry was with the National Research Council, NASA Ames Research Center, Moffett Field, CA 94035 USA. He is now with the Group Silicom, 31500 Toulouse, France.

G. P. Livingston and L. A. Morrissey are with the University of Vermont, Burlington, VT 05405-0088 USA.

S. L. Ustin and J. L. Syder are with the University of California, Davis, CA 95616 USA.

M. C. Diaz Barrios is with Hidrogeocol Ltda., Bogota, Colombia.

F.-M. Bréon is with CEA/DSM/LMCE, 91191 Gif sur Yvette, France.

M. M. Leroy is with MEDIAS-France, 31055 Toulouse Cedex, France.

J.-Y. Balois and M. Herman are with Laboratoire d'Optique Atmosphérique, U.S.T. de Lille, 59655-Villeneuve d'Ascq, France.

S. R. Shewchuk is with the Saskatchewan Research Council, Saskatoon, Saskatchewan, S7N2X8 Canada.

J. A. Stearn was with Johnson Controls Corporation, NASA Ames Research Center, Moffett Field, CA 94035 USA. He is now with Mr. Sprinkler Fire Protection Corporation in Roseville, CA 95661 USA.

S. E. Zedler was with the University of California, Davis, CA 95616 USA. She is now with the Scripps Institute of Oceanography, La Jolla, CA 92037 USA.

S. Bouffies-Cloche was with CEA/DSM/LMCE, 91191 Gif sur Yvette, France. She is now with CETP/IPSL, 78140 Vélizy, France.

Publisher Item Identifier 10.1109/TGRS.2002.800233.

field-of-view multispectral imaging sensor [21], [27]. The radiance imagery was acquired in the solar principal plane on July 21, 1994 at an altitude of 7.5 km along ten parallel flight lines (Fig. 1). Each flight line was flown toward or away from the solar azimuth direction. Concurrent data of surface wind speeds were collected at the Old Jack Pine test site, located between 1 and 15 km from the various flight lines [28]. Large-format color infrared aerial photographs (23 cm  $\times$  23 cm) were concurrently collected from the C-130 aircraft using a high spatial resolution Zeiss mapping camera with a 153 mm focal length lens. The aerial photographs, which had an equivalent ground spatial resolution better than 0.3 m, included the subsolar or specular direction.

During flight the POLDER images were collected at 10 s sampling intervals, in five spectral bands (443 nm, 550 nm, 665 nm, 865 nm, and 910 nm). The field of view was approximately  $\pm 53^\circ$  in the along-track dimension (in the principal plane) and  $\pm 45^\circ$  in the across-track direction. Overlap of adjacent images is between 92% and 94%.

### B. Data Analysis

POLDER was calibrated at Laboratoire d'Optique Atmosphérique in France in May 1994 prior to the field campaign. The data were collected as digital numbers proportional to scene radiance that were converted to normalized radiance by multiplying by  $\pi$  and dividing by the solar radiance at the top of the atmosphere. To improve band-to-band registration accuracy, the spatial resolution of each image was degraded by averaging  $3 \times 3$  pixel regions, increasing the pixel size from 50 m to approximately 150 m.

The POLDER lens exhibits very low geometric distortion, keeping the 150 m pixel size constant throughout each image. This means that the POLDER angular resolution for these data varies from approximately  $1.1^\circ$  at nadir to approximately  $0.6^\circ$  at  $43^\circ$  zenith view angle, the specular direction. The angular resolution of a BRDF (bidirectional reflectance distribution function) estimated from POLDER data representing a 150 m footprint pixel depends upon the rate at which the POLDER sensor samples that ground area—as well as the aircraft speed, its height above the ground, and the zenith view angle. For the results reported here, the angular resolution of POLDER data of one footprint varies from approximately  $12.4^\circ$  at nadir to approximately  $6.5^\circ$  in the specular direction.

During the 110-min. period required for measurement of all the flight lines, the solar zenith angle changed from  $45^\circ$  to  $37^\circ$ . To compensate for the changing specular direction and allow overlay of data collected at various times during the flight, the zenith view angle of each pixel was divided by the solar zenith at the time of data collection in order to obtain an approximate zenith view angle in degrees.

$$\text{approximate zenith view angle} = (42^\circ) \left( \frac{\text{zenith view angle}}{\text{solar zenith angle}} \right)$$

All classifications were performed using two bands defined in directional space rather than spectral space, using imagery from the red (665 nm) spectral band. The two directional bands, limited to zenith view directions in the principal plane, included

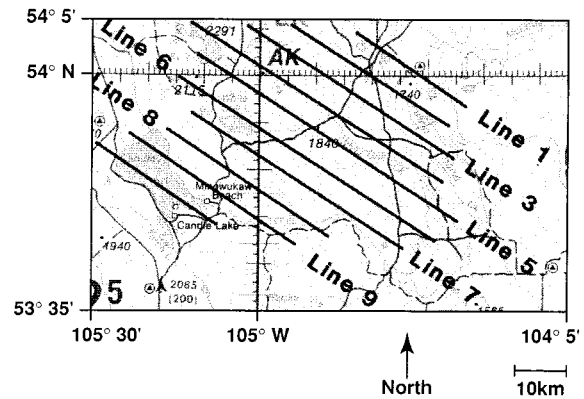


Fig. 1. On July 21, 1994, POLDER data were collected along parallel flight lines oriented approximately in the principal plane of the sun. The flight lines cover part of the Southern Study Area of the BOREAS Experiment located near Prince Albert, Saskatchewan, Canada. Image data from flight line 5 are shown in Fig. 5.

all data having a zenith view direction within  $\pm 2^\circ$  of the specular direction or within  $-4^\circ \pm 2^\circ$  ( $-2^\circ$  to  $-6^\circ$ ) from the specular direction. Data in directional space were classified, using a parallelepiped classifier, into three directional classes. The correspondence between the three directional classes and three information classes—open water, inundated vegetation, and non-inundated vegetation—was established by interpretation of the large-format aerial photographs.

Decision boundaries allowed classification of the data. A pixel was classified as “open water” if the normalized radiance in the  $-4^\circ$  directional band was greater than 0.1. For “noninundated vegetation,” the normalized radiance in the  $-4^\circ$  band was less than or equal to 0.1, and the normalized radiance in the specular directional band was less than 0.05. For “inundated vegetation,” the  $-4^\circ$  band normalized radiance was less than or equal to 0.1, and the specular band normalized radiance was greater than or equal to 0.05.

Interpretation of 11 color infrared air photographs, having approximately 60% overlap, collected along flight line 5 (Fig. 1) provided “ground truth” estimates of the fractions of open water, inundated vegetation, and other noninundated cover types in the principal plane of the flight line. Four analysts independently interpreted each photograph to estimate the type of ground cover present at 35 sample points located at the intersections of a  $5 \times 7$  rectangular grid of lines spaced 0.3 cm apart and oriented so that five lines were parallel to the principal plane. Only approximately 40% of the length of the flight line was photo-interpreted, because all photo-interpreted locations were within  $6^\circ$  of the specular direction, an angular range that included all sun glint from water (Table I).

The normalized difference vegetation index (NDVI) was computed

$$\frac{865 \text{ nm band} - 665 \text{ nm band}}{865 \text{ nm band} + 665 \text{ nm band}}$$

for the information classes—open water, inundated vegetation, noninundated vegetation 1, and noninundated vegetation 2—as a function of view angle in the principal plane. These information classes were identified using the directional not spectral space bands. Interpretation of the aerial photography suggested

TABLE I  
PROPORTION AND AREA OF COVER TYPES IN FLIGHT LINE

cover type	photo interpretation				Average	Classifier	
	A	B	C	D		- ha -	percent
inundated vegetation	18.6	19.2	18.8	20.0	19.2	135.	36.0
open water	10.2	9.0	9.1	9.7	9.5	67.0	11.4
non-inundated cover types	71.2	71.7	72.1	70.3	71.3	503.	52.6

that the two classes, noninundated vegetation 1 and noninundated vegetation 2, represented broad-leaf and needle-leaf vegetation, respectively.

The angular width of the specular peaks in the directional bands was estimated as either half the angular width at half of their maximum value (HWHM) or the full angular width at half their maximum value (FWHM).

### III. RESULTS

Fig. 2 shows the average normalized radiance of all classified pixels as a function of view angle for all flight lines. The average normalized radiance of noninundated cover types displays a maximum value of 0.046 in the hot spot direction, which is nearly an order of magnitude less than that measured in the specular direction of either inundated vegetation (0.24) or open water (0.58). The radiance of noninundated cover types displays a local maximum value in or near the specular direction, an unanticipated result possibly attributable to the presence of mixed pixels that contain at least some inundated vegetation and/or open water and that are classified—or misclassified—as noninundated cover types. Comparing only data collected in the specular direction, the average normalized radiances of inundated vegetation and open water areas are quite large, displaying values more than 8 and 19, respectively, times the average normalized radiance of noninundated cover types. The angular width of the specular peaks of inundated vegetation and open water areas are approximately 5° and 25°, respectively.

The resolution of Fig. 2, which is the average within 1° intervals along the horizontal axis of the bidirectional light-scattering properties of many ground areas, is limited by the angular resolution of the POLDER sensor, approximately 0.6° in the specular direction for the 150 m pixels used in this research. These results provide the incorrect impression that the angular resolution of the POLDER data of a *specific ground footprint* is better than its nominal 6.5° in this 42° zenith view direction. Fig. 2 may suggest, incorrectly, that the normalized radiance is zero for open water measured at zenith view angles between -60° and +5°, while in fact the values are nonzero but less than 0.01. There are no data values for zenith view angles between -80° and -60° and between 60° and 80°.

Data values in Fig. 2, at angles between 53° and 60°, are beyond the limit of the field of view of POLDER and occur because of an artifact introduced during data processing. The cause of the unrealistically abrupt decreases of the normalized

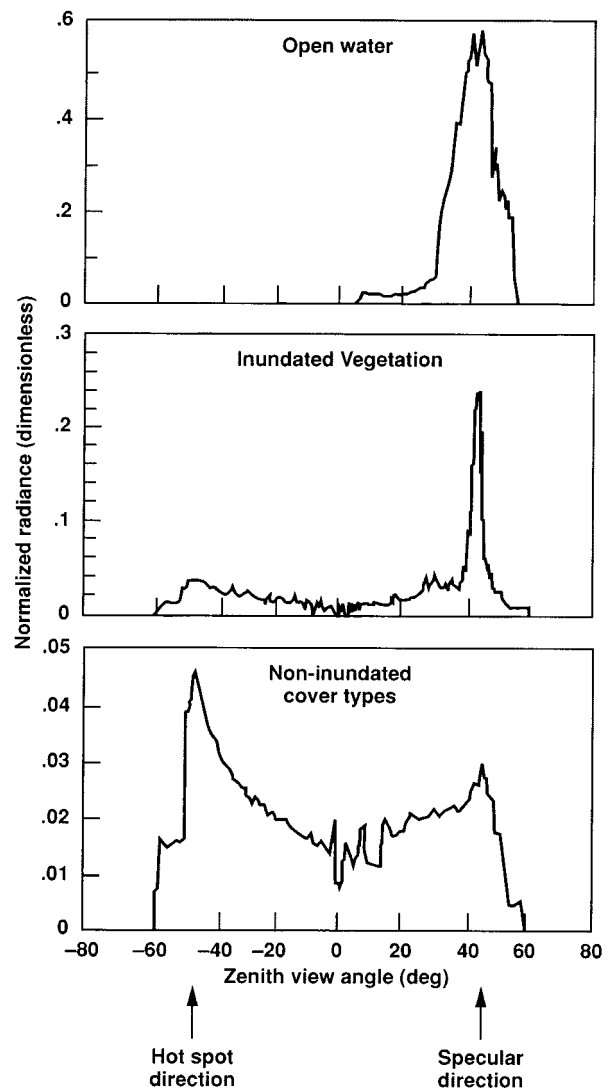


Fig. 2. The normalized radiance of three cover types measured in the red spectral region varied with view angle—being maximum in the specular direction for inundated vegetation and open water and in the hot spot direction for noninundated cover types. The noninundated cover types included primarily vegetation with very minor amounts of clear-cut area and asphalt road surface. The approximate zenith angle, the horizontal axis, is defined in Section II.

radiance (Fig. 2), which occur as view angles increase beyond approximately 55°, is not clear.

Fig. 3 shows that for most view angles, values of the NDVI of inundated vegetation are similar to the NDVI of noninundated

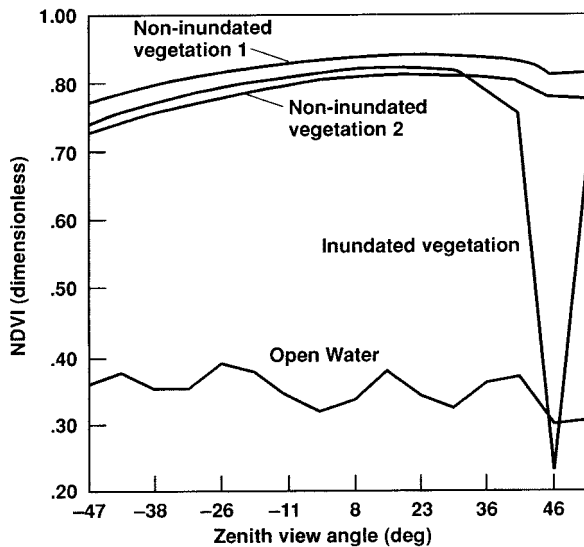


Fig. 3. The NDVI of various cover types varied with view angle, being less than 0.3 for inundated vegetation viewed in the specular direction. The four classes—noninundated vegetation 1, noninundated vegetation 2, inundated vegetation, and open water—were identified with the aid of a classification performed in spectral, not directional space as elsewhere in this article.

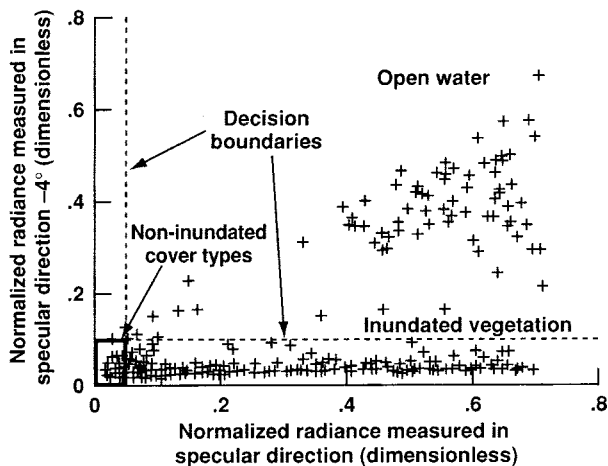


Fig. 4. A scatter diagram of normalized radiances in the red spectral region observed in two zenith view directions  $4^\circ$  apart reveals that the data cluster according to cover type.

vegetation, all being above approximately 0.75. The exception is the specular direction where NDVI is less than 0.30.

Fig. 4 shows all data collected in the two directional bands: specular and (specular  $-4^\circ$ ). Pixels representing open water areas, which appear bright in both these view directions, tend to be located in the upper right of Fig. 4. Pixels representing noninundated cover types, which appear dark in both of these view directions, are clustered just above zero on each axis. Pixels representing inundated vegetation, which appear bright in the specular direction but comparatively dark just  $4^\circ$  away from the specular direction, appear along a line just above the horizontal axis. Because of the patchy nature of the landscape evident in the aerial photographs, the 150 m diameter ground area repre-

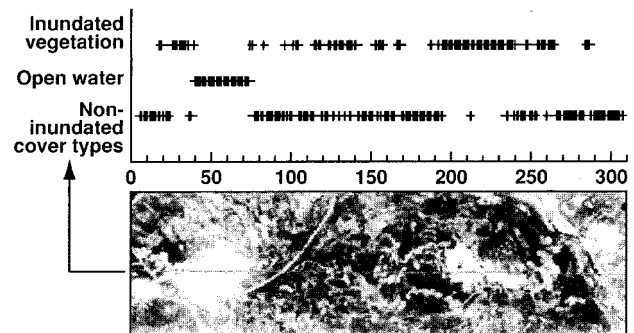


Fig. 5. Radiance data measured in the red wavelength region along the principal plane (which is approximately the center line of the flight line) were classified using a parallelepiped classifier applied to directional space rather than spectral space. The classification of each pixel is indicated by a corresponding mark in the appropriate row—inundated vegetation, open water, and noninundated cover types. Pixel count in the along-track direction varied by between 0 and 310.

sented by each pixel often includes more than one cover type. In the results, Fig. 4, data values representing these mixed pixels appear at locations between the three clusters of data points representing pure pixels and were identified with the three information classes: noninundated cover types, inundated vegetation, and open water.

Fig. 5 shows the classification map for a 150 m (one pixel) wide swath extending 47 km (310 pixels) along the principal plane of flight line 5 (see Fig. 1). All pixels classified as “open water” represent the lake (pixel numbers 40–75). Photo interpretation revealed no other open water areas within the classified area. Comparison of the air photos and classification results suggests that pixels (numbers 15–35) classified as inundated vegetation represent primarily inundated black spruce vegetation. In several instances, the pixels classified as inundated vegetation represent clear-cut areas (approximately 300 m across) containing small (5 m to 10 m across) open water areas. Photo interpretation results showed that the noninundated cover types class included vegetation primarily but also a small amount (approximately 4.8%) of clear-cut area. And interpretation of the air photos showed that pixels representing several small rivers and streams, located in the vicinity of pixel number 270, were classified as inundated vegetation.

Table I provides estimates obtained through classification and photo interpretation, revealing both the proportion and the area of the flight line representing inundated vegetation, open water, and noninundated cover types. The average of the estimates provided by the four photo interpreters (A, B, C, D) shows that 19.2% and 135 ha of the flight line were estimated to be inundated vegetation. In comparison, results obtained through use of the classification algorithm show that 36.0% and 254 ha of the flight line represented inundated vegetation. The area of the flight line was 47 km  $\times$  150 m or 705 ha.

Fig. 6 shows that sun glint from open water was observed within approximately  $10^\circ$  (HWHM) of the specular direction, given surface wind speeds of 2–4 m/s. In contrast, reflected sun glint from calm water surfaces, such as typically found beneath inundated vegetation, was observed only within about  $2.5^\circ$  (HWHM) of the specular direction.

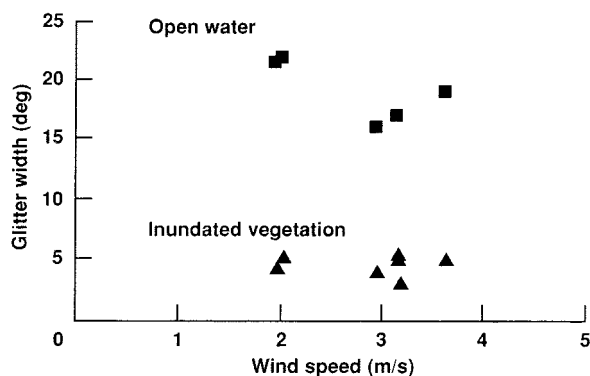


Fig. 6. The angular widths of the specular peaks representing inundated vegetation were less than approximately  $5^\circ$ , while those representing open water areas were greater than approximately  $15^\circ$ —regardless of wind speed. Angular width was measured at one half of the maximum value of the specular peak (FWHM) (Fig. 2).

#### IV. DISCUSSION

##### A. Glitter Allows Discrimination of Inundated Areas

The area of inundation, which may be estimated using our approach, is key to addressing scientific questions related to carbon, energy, and water budgets. As such, it provides information about functions and functioning of wetlands. The area of inundation provides information on wetlands hydrology, one of nine key parameters important for characterizing the role of wetlands in biogeochemical cycling of trace substances [4]. Our approach appears readily extendable to multitemporal analyses of seasonal and interannual distributions of inundation, potentially providing information critical to gaining a better understanding of carbon, water, and energy budgets, especially those representing high-latitude ecosystems where climatic change is expected to dramatically alter regional surface hydrology.

Multitemporal estimates of the inundation area may aid in the delineation of wetlands, a legally important process in the United States because of federal regulatory statutes [6], [29]. While our approach allows identification of areas inundated on one date, our approach does not allow direct delineation of wetlands, since inundated areas are not necessarily wetlands. By itself, observation of inundation on one date indicates only a hydrological event and not the duration and frequency of that event, two of the several factors linked to the presence of a hydric substrate and hydrophytic vegetation [5], the criteria defining a wetland [5], [6]. Occasional flooding does not distinctively separate wetlands from uplands, many of which flood occasionally [6]. However, our approach, if augmented to include analysis of an ensemble of remotely sensed images collected over the growing season, presumably would provide data on the duration, frequency, and timing of inundation.

Our results demonstrate that differences in the directional signature of open water, inundated vegetation, and noninundated cover types allow their discrimination and classification (Fig. 5). In the specular direction, water reflects sunlight significantly better than other cover types. Both open water and inundated vegetation provide a large, wavelength-independent, sun glint signature that differs greatly from the radiance of noninundated areas. In directions away from the specular direction, sun glint from open water areas may persist, depending upon the size and

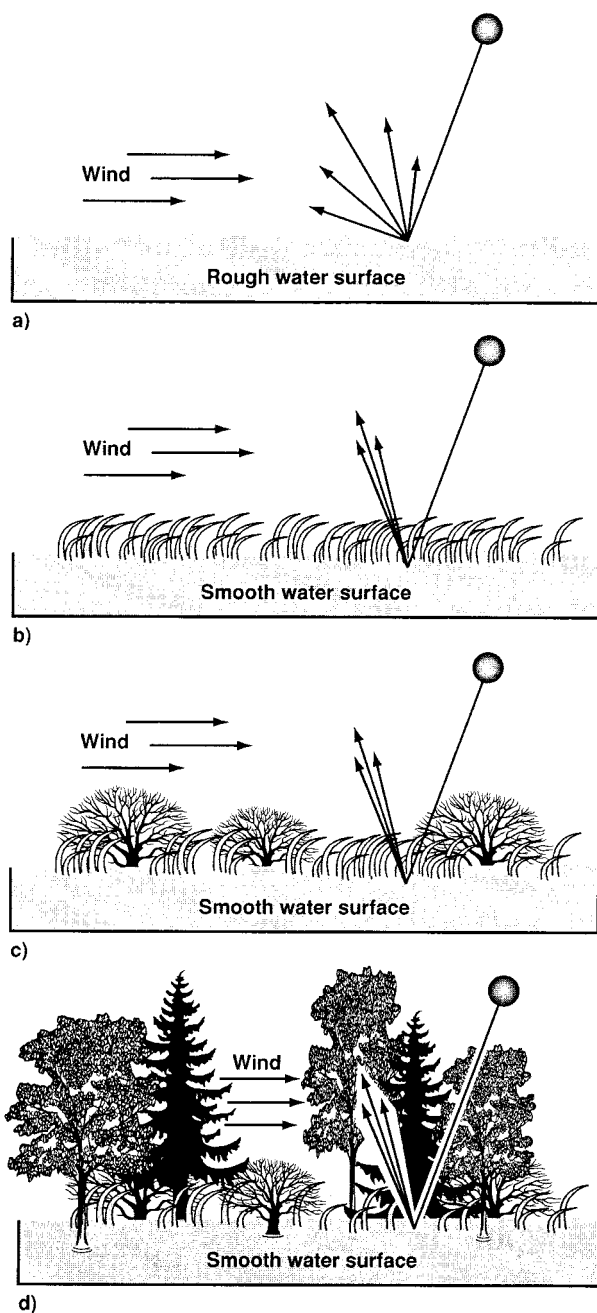


Fig. 7. We tested the hypothesis that inundated vegetation and open water areas will appear differently in remotely sensed data collected with view direction. (a) Wind readily ruffles an open water surface, which scatters incident radiation over a broad range of view directions. Conversely, a water surface reflects sunlight over a more limited range of view directions when it is sheltered by (b) inundated emergent herbaceous vegetation, (c) inundated woody shrubs, and (d) an inundated black spruce forest.

direction of the wind-driven waves (Fig. 7) [24], [25]. In this study, the angular size of the specular lobe of the sun glint from the wind-ruffled open water areas was approximately four times [ $10^\circ$  compared to  $2.5^\circ$  (HWHM)] that from calm water surfaces typically found beneath inundated vegetation. Thus, discrimination of these two cover types depended solely upon their differing directional signatures and not upon their spectral signatures, which sometimes were identical within the error of the measurements.

## B. Validity of Hypotheses

### First Hypothesis:

*The glitter of sunlight off water surfaces provides a strong, angular signature reflection characteristic of inundated areas and uncharacteristic of other, noninundated cover types.*

This hypothesis is supported by Figs. 2–6, which demonstrate that the normalized radiances of open water and inundated vegetation are generally much larger than those of noninundated cover types and show large variation with view angle. Such properties are uncharacteristic of the specular reflecting properties of plant canopies [30], [31]. Measurements [30] in the red spectral region of plant canopies having nonplanophyll leaf angle distributions show that the specular portion of the light scattered in a specific view direction is consistently less than 50% of the total light scattered in that direction by the canopy. We observed no planophyll canopies in the study area. All of this suggests that in general—and specifically for these results (Figs. 2–6)—it is probable that glitter from noninundated, nonplanophyll vegetative cover types is insignificant compared to glitter from open water and inundated vegetation. We believe our first hypothesis is valid for nonplanophyll canopies in nonfrozen wetlands.

### Second Hypothesis:

*Inundated wetlands and open water areas display different, wind-dependent glitter signatures as a function of view angle.*

This hypothesis, illustrated in Fig. 7, is supported by the results (see Table I and Fig. 6). For the intermediate wind speeds 2–4 m/s measured during image data collection, the angular spread of the glitter from open water areas was greater than that from inundated vegetation. At these wind speeds, the wind-sheltering effects of the emergent vegetation allowed separation of inundated vegetation and open water in the POLDER data. Thus, the second hypothesis appears correct for the intermediate range of wind speeds measured during image data collection. Presumably, the second hypothesis would fail as wind speed approaches zero or, conversely, as wind speed increases beyond the range for which the vegetation shelters the water surface.

### Third Hypothesis:

*Analysis of remotely sensed data, collected in and near the specular direction, will allow accurate discrimination of inundated wetlands, open water, and noninundated cover types.*

This hypothesis is supported by Fig. 5 and Table I. Comparisons between the results (Table I) obtained by classification and by photo interpretation of the flight line are encouraging, but our approach appears to have significantly overestimated the areal extent of inundated vegetation. We attribute this error to use of a parallelepiped classification algorithm that employed thresholds in directional space as decision boundaries, to the presence of mixed pixels and to errors in photo interpretation. A less-than-optimally-selected threshold value is a possible explanation for the semblance of a specular peak in the average radiance representing noninundated cover types (Fig. 2). Presumably, application of a more sophisticated classification algorithm encompassing not only directional space but also spectral space and polarization space would provide improved results for classification of inundated vegetation.

Our apparent overestimation of inundation (Table I) was also possibly due in part to treating mixed pixels as if they were homogeneous. A successful mixture analysis, perhaps one in which the directional information employed in this analysis is supplemented with spectral information, presumably would allow estimation of the fraction of each cover type within each pixel, leading to improved estimates of the areal extent of each cover type for the flight line.

We suspect our photo interpretation. In addition to the usual generic sources of error commonly found in results obtained through photo interpretation, our interpretation results may be biased due to flare in the lens and film used to image the very bright sun glint against a much darker background of foliage, litter, and shadowed water. Finally, the differences (Table I) may be due to the fact that different areas of the flight line were represented in the 11 photographic images of the sun glint as compared to the 50 POLDER images of the sun glint.

Except for small areas of open water and several small rivers and streams misclassified as inundated vegetation and excepting the overestimation of inundated vegetation, the classification results (Fig. 5) appear in good agreement with Table I, obtained from a wetlands map of the flight line that was developed by photo-interpreting the 11 large-format aerial photographs. Misclassification of small rivers and small open water areas as inundated vegetation is thought in part due to the wind-sheltering effects of nearby tall woody vegetation.

## C. Wetlands Classification Using Sun Glint

These results demonstrate that classification of the glitter is possible if and only if a ground region has been observed in or near the specular direction in the principal plane. If not, then naive application of the classifier may provide errors of omission; inundated vegetation may be present but presumably would not be detected.

## D. Normalized Difference Vegetation Index

Our results (Fig. 3) suggest that NDVI, when estimated both in the specular direction and away from the specular direction, will provide a metric sensitive to detection of inundated vegetation. In directions away from the specular direction, the signatures of noninundated cover types and of inundated vegetation appear similar, each having a local maximum in the hot spot direction. NDVI values are low in the specular direction because the glitter from the water surface of the inundated vegetation is large in both the red and near infrared wavelength bands, yielding NDVI values close to zero.

## E. Other Sources of Variability

Pure pixels within the open water cluster (Fig. 4) appear somewhat dispersed rather than tightly clumped about one location, presumably due both to differences in the interaction process between wind and the water surface as well as to the effects of misregistration between bands in directional space. The differences in the wind–water interaction process may depend in part upon the geographical size and depth of the open water area and upon the sheltering provided by nearby vegetation and land forms. Taking these differences

into account suggests that the size of the specular lobe of open water may at times be much less than  $30^\circ$  in which case the data would likely be dispersed as in this study.

Misregistration between the two directional bands of Fig. 4 may also be important for understanding the dispersion of the data representing open water. For measurements of open water having a  $30^\circ$  specular lobe, data in the two directional bands—which are only  $4^\circ$  apart—should be highly correlated. However, increasing amounts of misregistration will tend to reduce the correlation between bands, changing the dispersion of the data from an elongated shape toward the origin to the more rounded cluster of pure open-water pixels evident in Fig. 4. The amount of misregistration between these two bands varied from zero to a maximum of approximately 0.5 pixels, depending upon the specific location along the flight line. The decorrelation effects provided by the misregistration of these two directional bands presumably are similar to decorrelation effects due to misregistration between two spectral bands [32].

The inundated vegetation line segment (Fig. 4) terminated by pure pixel clusters representing, respectively, inundated vegetation and noninundated cover types presumably includes along its length mixed pixels representing varying proportions of these two classes. In addition, however, the spread of the data points along the inundated vegetation line may represent a second potential source of variation due to the light-transmitting properties of the emergent vegetation. As a consequence, the ground footprint of some pixels located along the inundated vegetation line may include only inundated vegetation, not a mixture of inundated vegetation and noninundated cover types. The varying amounts of vegetation emergent above the water surface will correspondingly reduce the magnitude of the direct beam sunlight, a magnitude represented by a position along the inundated vegetation line, that successfully traverses the canopy twice—from the sun to the water surface and from the water surface to the sensor. The effect increases with decreasing solar elevation. If the canopy intercepts little direct beam sunlight, then the corresponding data point would be located close presumably to the end of the line near the inundated-vegetation pure pixels. Conversely, data points representing a canopy that intercepts most direct beam sunlight would be located presumably at the other end of the line near the pure pixels of noninundated cover types. In other words the inundated vegetation line presumably includes along its length some pure inundated vegetation pixels.

The scatter of data along the inundated vegetation line (Fig. 4) may also represent a third potential source of variation due to undersampling of inundated vegetation. The POLDER sensor measured the radiance peak of inundated vegetation, which is approximately  $5^\circ$  wide (FWHM), sampling with an angular resolution of approximately  $6.5^\circ$ . This means that few samples represent the maximum radiance of the inundated vegetation—and that most data values representing inundated vegetation appear at intermediate values along the inundated vegetation line segment.

## V. CONCLUSIONS

We have developed a new remote-sensing technique for identifying inundated areas based on the properties of the glitter—the strong, angular signature reflection that is characteristic of

surface water and uncharacteristic of other cover types. We discriminated three cover types—vegetation emergent above inundated soils, open water, and noninundated cover types—from analysis of directional data, not spectral data, collected by the airborne POLDER sensor. Application of our new technique holds promise for mapping the seasonal and interannual extent of inundation, a key descriptor of wetlands hydrology.

## ACKNOWLEDGMENT

We would like to acknowledge the thoughtful comments of the anonymous reviewers of this article, the NASA Terrestrial Ecology Program, and the Ames Research Center. We would also like to acknowledge the support for operation of the POLDER instrument and for POLDER data processing provided by Laboratoire d'Optique Atmosphérique, U.S.T. de Lille, Lille, France, by Laboratoire de Modelization du Climat et de l'Environnement, CEA/DSM, Gif sur Yvette, France, and by Centre d'Etudes Spatiales de la Biosphère (CESBIO), UMR CNES-CNRS-UPS, Toulouse, France. Finally, we would like to acknowledge the support of the Saskatchewan Research Council, Saskatoon, Saskatchewan, Canada.

## REFERENCES

- [1] R. W. A. Hutjes, P. Kabat, S. W. Running, W. J. Shuttleworth, C. Field, B. Bass, M. A. F. D. Dias, R. Avissar, A. Becker, M. Claussen, A. J. Dolman, R. A. Feddes, M. Fosberg, Y. Fukushima, J. H. C. Gash, L. Guenni, H. Hoff, P. G. Jarvis, I. Kayane, A. N. Krenke, C. Liu, M. Meybeck, C. A. Nobre, L. Oyebande, A. Pitman, R. A. Pielke, M. Raupach, B. Saugier, E. D. Schulze, P. J. Sellers, J. D. Tenhunen, R. Valentini, R. L. Victoria, and C. J. Vorosmarty, "Biospheric aspects of the hydrological cycle: Preface," *J. Hydrol.*, vol. 213, pp. 1–21, 1998.
- [2] J. Slanina, P. Warneck, N. M. Bazhin, H. Akimoto, W. M. Kieskamp, M. A. K. Khalil, J. G. Calvert, E. Matthews, L. Barrie, M. Wahlen, S. E. Schwartz, X. Tang, and O. N. Singh, "Assessment of uncertainties in the projected concentrations of methane in the atmosphere," *Pure Appl. Chem.*, vol. 66, pp. 137–200, 1994.
- [3] W. C. Oechel and G. L. Vourlitis, "The effects of climate-change on land atmosphere feedback in arctic tundra regions," *Trends Ecol. Evol.*, vol. 9, pp. 324–329, 1994.
- [4] D. Sahagian and J. Melack, "IGBP Report 46: Global wetland distribution and functional characterization: Trace gases and the hydrologic cycle report from the Joint GAIM, BAHC, IGBP-DIS, IGAC and LUCC Workshop," Santa Barbara, CA, D. Sahagian and J. Melack, Eds., 1996.
- [5] R. W. Tiner, *Wetland Indicators: A Guide to Wetland Identification, Delineation, Classification and Mapping*. Boca Raton, FL: Lewis, 1999.
- [6] NRC, *Wetlands Characteristics and Boundaries*. Washington, DC: National Academy, 1995.
- [7] L. A. Morrissey and G. P. Livingston, "Methane emissions from Alaska Arctic tundra: An assessment of local spatial variability," *J. Geophys. Res.*, vol. 97, pp. 16661–16670, 1992.
- [8] B. P. Walter and M. Heimann, "A process-based, climate-sensitive model to derive methane emissions from natural wetlands: Application to five wetland sites, sensitivity to model parameters and climate," *Global Biogeochem. Cycles*, vol. 14, pp. 745–765, 2000.
- [9] W. R. Rouse, "A water balance model for a subarctic sedge fen and its application to climatic change," *Clim. Change*, vol. 38, pp. 207–234, 1998.
- [10] P. M. Lafleur, J. H. McCaughey, D. W. Joiner, P. A. Bartlett, and D. E. Jelinski, "Seasonal trends in energy, water and carbon dioxide fluxes at a northern boreal wetland," *J. Geophys. Res. Atmos.*, vol. 102, pp. 29009–29020, 1997.
- [11] L. D. Boudreau and W. R. Rouse, "The role of individual terrain units in the water-balance of wetland tundra," *Clim. Res.*, vol. 5, pp. 31–47, 1995.
- [12] D. A. Wessel and W. R. Rouse, "Modeling evaporation from wetland tundra," *Boundary-Layer Meteorol.*, vol. 68, pp. 109–130, 1994.
- [13] S. D. Bridgman, J. Pastor, K. Updegraff, T. J. Malterer, K. Johnson, E. Harth, and J. Q. Chen, "Ecosystem control over temperature and energy flux in northern peatlands," *Ecol. Appl.*, vol. 9, p. 1345, 1999.

- [14] E. Matthews and I. Fung, "Methane emission from natural wetlands: Global distribution, area and environmental characteristics of sources," *Global Biogeochem. Cycles*, vol. 1, pp. 61–86, 1987.
- [15] K. B. Bartlett and R. C. Harriss, "Review and assessment of methane emissions from wetlands," *Chemosphere*, vol. 26, pp. 261–320, 1993.
- [16] A. S. Belward, J. E. Estes, and K. D. Kline, "The IGBP-DIS global 1-km land-cover data set DISCover: A project overview," *Photogram. Eng. Rem. Sens.*, vol. 65, pp. 1013–1020, 1999.
- [17] L. A. Morrissey, G. P. Livingston, and S. L. Durden, "Use of SAR in regional methane exchange studies," *Int. J. Rem. Sens.*, vol. 15, pp. 1337–1342, 1994.
- [18] E. S. Kasischke, J. M. Melack, and M. C. Dobson, "The use of imaging radars for ecological applications: A review," *Rem. Sens. Environ.*, vol. 59, pp. 141–156, 1997.
- [19] S. V. Muller, A. E. Racoviteanu, and D. A. Walker, "Landsat MSS-derived land-cover map of northern Alaska: Extrapolation methods and a comparison with photo-interpreted and AVHRR-derived maps," *Int. J. Rem. Sens.*, vol. 20, pp. 2921–2946, 1999.
- [20] D. Muchoney, A. Strahler, J. Hodges, and J. Lo Castro, "The IGBP DIS-Cover confidence sites and the system for terrestrial ecosystem parameterization: Tools for validating global land-cover data," *Photogram. Eng. Rem. Sens.*, vol. 65, pp. 1061–1067, 1999.
- [21] F.-M. Bréon, V. Vanderbilt, M. Leroy, P. Bicheron, C. L. Walthall, and J. E. Kalshoven, "Evidence of hot spot directional signature from airborne POLDER measurements," *IEEE Trans. Geosci. Remote Sensing*, vol. 35, pp. 479–484, Mar. 1997.
- [22] P. Sellers, F. Hall, H. Margolis, B. Kelly, D. Baldocchi, G. d. Hartog, J. Cihlar, M. G. Ryan, B. Goodison, P. Crill, K. J. Ranson, D. Lettenmaier, and D. E. Wickland, "The boreal ecosystem-atmosphere study (BOREAS): An overview and early results from the 1994 field year," *Bull. Amer. Meteorol. Soc.*, vol. 76, pp. 1549–1577, 1995.
- [23] P. Sellers, F. Hall, R. D. Kelly, A. Black, D. Baldocchi, J. Berry, M. Ryan, K. J. Ranson, P. M. Crill, D. P. Lettenmaier, H. Margolis, J. Cihlar, J. Newcomer, D. Fitzjarrald, P. G. Jarvis, S. T. Gower, D. Halliwell, D. Williams, B. Goodison, D. E. Wickland, and F. E. Guertin, "BOREAS in 1997: Experiment overview, scientific results and future directions," *J. Geophys. Res. Atmos.*, vol. 102, pp. 28731–28769, 1997.
- [24] C. Cox and W. Munk, "Measurements of the roughness of the sea surface from photographs of the sun's glitter," *J. Opt. Soc. Amer.*, vol. 44, pp. 838–850, 1954.
- [25] F.-M. Bréon and P.-Y. Deschamps, "Optical and physical parameter retrieval from POLDER measurements over the ocean using an analytical model," *Rem. Sens. Environ.*, vol. 43, pp. 1–20, 1992.
- [26] M. Leroy and F.-M. Bréon, "Surface reflectance angular signatures from airborne POLDER data," *Rem. Sens. Environ.*, vol. 57, pp. 97–107, 1996.
- [27] P.-Y. Deschamps, F.-M. Bréon, M. Leroy, A. Podaire, A. Bricaud, J.-C. Buriez, and G. Seze, "The POLDER mission: Instrument characteristics and scientific objectives," *IEEE Trans. Geosci. Remote Sensing*, vol. 32, pp. 598–615, May 1994.
- [28] S. R. Shewchuk, "Surface Mesonet for BOREAS," *J. Geophys. Res. Atmos.*, vol. 102, pp. 29077–29082, 1997.
- [29] T. A. Gress, D. Kettler, C. Mao, L. Wright, and S. Berta, "Wetland recertification and sampling using satellite remote-sensing," *Adv. Space Res.*, vol. 13, pp. 83–90, 1993.
- [30] V. C. Vanderbilt, L. Grant, and S. L. Ustin, "Polarization of light by vegetation," in *Photon-Vegetation Interactions, Applications in Optical Remote Sensing and Plant Ecology*, R. Myneni and J. Ross, Eds. Berlin, Germany: Springer-Verlag, 1990, pp. 194–228.
- [31] G. Rondeaux and M. Herman, "Polarization of light reflected by crop canopies," *Rem. Sens. Environ.*, vol. 38, pp. 63–75, 1991.
- [32] P. H. Swain, V. C. Vanderbilt, and C. D. Jobusch, "A quantitative applications-oriented evaluation of thematic mapper design specifications," *IEEE Trans. Geosci. Remote Sensing*, vol. 20, pp. 370–377, 1982.



**Vern C. Vanderbilt** (M'77) received the B.S., M.S., and Ph.D. degrees in electrical engineering from Purdue University, West Lafayette, IN, after which he held a Postdoctoral Fellowship and was an Engineer at Purdue's Laboratory for Applications of Remote Sensing (LARS).

After serving as a scientist with TGS Technology, Moffett Field, CA, he joined the NASA Ames Research Center, Moffett Field, CA where his research involves the polarized light-scattering properties of leaves, plants, and, most recently, wetlands. He served on NASA's MODIS Science Team from 1988

to 1995 and now serves on CNES's POLDER II Science Team.



**Guillaume L. Perry** received the Engineer Diploma in electronics from Institut Supérieur d'Electronique du Nord, Lille, France in 1991 and the Ph.D. degree in 1996 from the Université des Sciences et Techniques de Lille (U.S.T.L.) Flandres Artois, Villeneuve d'Ascq, France. His thesis research involved development of techniques for remotely sensing atmospheric aerosol properties using the POLDER radiometer.

Between 1996 and 1998, he was a Postdoctoral Fellow with the National Research Council at the NASA Ames Research Center, Moffett Field, CA investigating the detection of wetlands in POLDER data, concentrating on their specularly reflecting properties. Upon returning to France, he completed his research on remote sensing of atmospheric aerosols at U.S.T.L. before beginning work in informatics. He is now with the Group Silicom in Toulouse, France.

**Gerald P. Livingston** received the Ph.D. degree from Texas A&M University in biology/ecology in 1981.

He was a Senior Research Scientist at NASA's Johnson Space Center, Houston, TX and Ames Research Center, Moffett Field, CA before becoming a Research Associate Professor at the University of Vermont, Burlington. His research has involved the application of remote sensing to a variety of environmental and earth system areas, including agricultural, disease vector, and biogeochemical dynamics. His research interests are application of advanced optic and microwave sensors to monitor surface hydrologic dynamics in northern high-latitude ecosystems in pursuit of improving soil carbon dynamic models in view of climatic change.

Dr. Livingston is a member of the POLDER, ENVISAT, and ALOS international investigator's science teams.



**Susan L. Ustin** (M'90) received the B.S. and M.S. degrees in biology from California State University, Hayward and the Ph.D. degree in botany from the University of California, Davis in 1983 in the area of plant physiological ecology.

She is a Professor of resource science in the Department of Land, Air and Water Resources at University of California, Davis. She is also Director of the California Space Institute Center of Excellence at the University of California and the Center for Spatial Technologies and Remote

Sensing (CSTARS) and Associate Director of the United States Department of Energy's Western Regional Center for Global Environmental Change. She has served on several National Research Council and NASA committees. Her research interests are remote-sensing applications in many different ecological communities, particularly using imaging spectrometry and other new sensing technologies. She has authored more than 150 papers and reports on these subjects.

**Martha C. Diaz Barrios** received the M.S. degree in hydrology at the University of California, Davis in 1997. Her thesis is related to some aspects of this publication. She earned the M.E. degree in water resources (1993) and a B.S. degree in civil engineering (1991) from the University of Los Andes, Bogota, Colombia. She is currently employed as a hydrologic engineer for Hidrogeocol Ltda in Bogota, Colombia.



**François-Marie Bréon** received the Ph.D. degree from the University of Paris, France in 1989. His doctoral thesis focused on the use of infrared sounders for the retrieval of water vapor and temperature atmospheric profiles.

After postdoctoral positions at the California Space Institute, San Diego, CA and the Laboratoire d'Optique Atmosphérique, Villeneuve d'Ascq, France he joined the Laboratoire des Sciences du Climat et de l'Environnement, Gif-Sur-Yvette, France in 1993 to lead the scientific analysis of spaceborne

POLDER measurements. His research interests are the use of spectral, directional, and polarization signatures of the measured reflectances for atmospheric and surface monitoring from space. He is a Principal Investigator for several satellite missions. He has authored and coauthored more than 30 papers in peer-reviewed journals.

**Marc M. Leroy** obtained the Ph.D. degree at the Paris VII University, France in 1980 in the field of radiatively driven stellar winds.

He became a Research Associate at the Observatoire de Paris, France in 1981 and worked in the field of theoretical plasma physics of the earth's bow shock. He joined the French Space Agency (Centre National d'Etudes Spatiales) in Toulouse, 1985, to work on calibration activities associated with the SPOT and other programs. He joined LERTS/CESBIO in 1993 with a specific interest in the physics of remote-sensing measurements in the optical domain. He is presently at MEDIAS-France, Toulouse in charge of the development of algorithms for land surface biophysical and geophysical products from POLDER. He has authored over 50 peer-reviewed papers or book articles in the scientific literature.



**Jean-Yves Balois** received the B.A. degree in engineering at Conservatoire National des Arts et Métiers, Lille, France in 1985.

Currently, he is a Research Engineer in the Laboratoire d'Optique Atmosphérique, Villeneuve d'Ascq, France. He joined the Centre National de la Recherche Scientifique working at the Université des Sciences et Technologies de Lille, Lille, France, in 1992 where he is in charge of the airborne POLDER simulator and other radiometers developed at Laboratoire d'Optique Atmosphérique.

**Leslie A. Morrissey** received the Ph.D. degree from Oregon State University, Corvallis, OR and undergraduate degree from San Jose State University, San Jose, CA.

She is an Associate Professor at the School of Natural Resources, University of Vermont, Burlington. Her current research interests are the use of satellite data (microwave and optical) and geographic information systems for mapping and monitoring wetlands and water quality. Previously, as a Senior Research Scientist at NASA Ames Research Center, Moffet Field, CA her research centered on the use of SAR data for monitoring environmental controls on methane exchange in northern ecosystems. Since 1976, her research at Ames Research Center involved the use and assessment of remote-sensing technologies for environmental applications in California and Alaska.



**Stanley R. Shewchuk** graduated in 1974 from the University of Toronto as a forecast meteorologist. He has extensive experience with atmospheric processes involving droplet cloud physical interactions. Since graduation, he has worked for the Saskatchewan Research Council, Saskatoon, Saskatchewan, Canada focusing on atmospheric sciences program structures of relevance to the province of Saskatchewan. Areas of expertise include air quality dispersion modeling, open path techniques, mass flux programs, pesticide droplet drift, surface meteorology programs, and

cloud physics via weather modification. His involvement with the recent NASA Boreas project dealt with the establishment of the surface meteorology infrastructure.

**Joel A. Stearn** received the B.S. degree in management of information systems from California State University, Hayward in 1987. He served as a Research Assistant at NASA Ames Research Center, Moffet Field, CA while studying for an M.S. degree in environmental studies at California State University, San Jose with a focus in remote sensing. His research centered on the use of SAR data and optical sensors for monitoring environmental controls and wetland mapping in northern ecosystems. Currently, he is the Chief Financial Officer for Mr. Sprinkler Fire Protection Corporation in Roseville, CA.



**Sarah E. Zedler** received the B.S. degree in physics from the University of California, Davis in 1996 and received the M.S. degree in geography from the University of California, Santa Barbara in 1999. She is currently pursuing a Ph.D. degree in physical oceanography at Scripps Institute of Oceanography, La Jolla, CA.



**Jonathan L. Syder** received the B.S. degree in natural sciences and the B.S. in anthropology from University of Alaska, Anchorage. He is pursuing the Ph.D. degree at the University of California, Davis, conducting remote-sensing research on albatross foraging patterns related to surface oceanography.



**Sophie Bouffies-Cloche** received the Ph.D. degree in 1996 from the University of Paris, France. Her doctoral thesis focused on the use of POLDER for the retrieval of water vapor and detection of clouds.

After postdoctoral positions at the Laboratoire de Météorologie Dynamique du C.N.R.S., Palaiseau, France and the Centre d'étude des Environnements Terrestre et Planétaires, Saint-Maur-des-Fossés, France in 2001 she joined the Institut Pierre Simon Laplace, Vélizy, France to manage scientific databases.



**Maurice Herman** received the M.S. degree in 1962 and the Ph.D. degree in 1968 both from the University of Lille, France.

He has been a Professor of physics since 1969 and has been involved in the design and interpretation of several balloon-borne and spaceborne remote-sensing experiments. His research interests are atmospheric radiative transfer modeling, interpretation of satellite imagery and other remote-sensing measurements, and monitoring of atmospheric aerosols properties, with emphasis on polarization. He is heavily involved in the POLDER experiment, in particular for the instrument vicarious calibration and the remote sensing of aerosols.